Chemical Conditions Affecting Iron Oxides:

Does the presence of phosphate within the structure of the iron oxides make them less reducible than synthetic pure ferrihydrite?

Samantha Shulman

7758198

July 15th 2015

Institute of the Environment at the University of Ottawa in partial fulfillment of the requirements of the MSc. Degree

EVD 6999

Supervisor: Dr. Danielle Fortin

Table of Contents

Abstract

The purpose of this study was to explore the redox stability of biogenic iron oxides and the implications for wastewater treatment. Specifically, we investigated if the presence of phosphate within the structure of ferrihydrite (an iron oxide) makes it less reducible (by iron reducing bacteria) than pure synthetic ferrihydrite. Experiments were conducted on four different synthetic ferrihydrite samples to determine the rates of ferric reduction by *Shewanella putrefaciens* CN32, a well-known iron reducing bacterium. The samples were: pure ferrihydrite, ferrihydrite and added alginate, ferrihydrite with 1 uM phosphate and a combination of the latter two. Our results showed that the addition of phosphate stabilized the ferrihydrite and slowed down the reduction process. Rates of reduction in mM Fe(II) per day were 0.0141 (ferrihydrite + alginate + PO_4), 0.0423(ferrihydrite + PO_4), 0.061(Ferrihydrite) and 0.0774 (ferrihydrite + alginate). This experiment confirms that sorbed phosphate onto ferrihydrite increases it redox stability, but its use as water treatment (to remove PO_4 or other contaminants in waste waters), should take in account the potential for microbial reduction, especially if the iron oxide sludge is disposed of in landfills.

List of Figures

List of Tables

Acknowledgements

I would like to thank my supervisor, Dr. Danielle Fortin, for taking me on as a student. She was extremely helpful throughout the short time period I had to do my research. Her advice on scientific research and writing has helped me advance both my knowledge and my confidence in the field.

My work could not have been completed without the long-distance support of my family. Countless phone calls and text messages were always answered and dollar bills always provided. Thank you Mala, Jeff and Shari. The students and staff of University of Ottawa's Institute of the Environment have afforded me with ongoing support throughout my degree, and especially during this project. Thank you for always scheduling around my lab work.

Finally, I would like to thank Brandon Khan and Tarek Najem-two incredibly smart and helpful Master's students that guided me through the process of my project. They taught me how to conduct experiments, provided me with resources and answered countless questions. I could not of done it without you two.

Thank you!

Introduction

The Earth is composed of many different elements and compounds, which makes it a diverse and complex place geochemically. The fourth most abundant element in Earth's crust is iron, and it is of important attention because it specifically contributes to many different processes on the Earth's surface (Fortin & Langley 2005; Langley et al., 2009), such as the formation of iron minerals and its involvement in microbial metabolism (Cornell and Schwertmann 2003; Lovely 1993;). As iron mainly exists in two oxidation states, ferrous iron(II) or ferric iron(III), it can be soluble under reducing conditions or insoluble under oxidizing conditions (Fortin & Langley 2005). In oxygenated environments, Fe(II) can be oxidized by both oxygen and microorganisms and precipitate as iron oxides.

Iron oxides are extensively present in nature throughout all spheres of the Earth (Cornell and Schwertmann 2003). Langley et al., (2009) state this is because both iron and atmospheric oxygen are existent nearly everywhere on the Earth's surface. They are composed of the elements iron, with oxygen and/or hydroxide. There are a total of sixteen different iron oxides (Cornell and Schwertmann, 2003). Ferrihydrite ($Fe_5O_8H.nH_2O$) is an iron oxide of poor crystalline structure (Cornell and Schwertmann 2003), it exists in the Fe(III) oxidation state (Kappler & Straub 2005) and can be categorized as a hydrous ferric oxide(HFO). Ferrihydrite is widespread in many natural environments that have a circumneutral pH (Kappler & Straub 2005), such as freshwater lakes, rivers, and sediment ponds (Fortin & Langley 2005; (Paige, Snodgrass, Nicholson, Scharer & He 1997). A specific property that Kappler and Straub (2005) state is that ferrihydrite and other iron oxides possess a positive net charge at a neutral pH.

Protonated and/or deprotonated binding sites on the iron oxides can bind negatively and/or positively charged ions, respectively. The iron oxides therefore act as sorbents (Kappler & Straub 2005), by having the adsorbing species interact with the surface hydroxyl groups on the iron oxide (Cornell & Schwertmann 2003). Phosphate, bicarbonate, oxyanions of toxic metals and organic matter can bind to the surface of the oxides (Kappler & Straub 2005). Another important property of iron oxides is that they have a high specific surface area (Cornell & Schwertmann, 2003). Because of their sorptive properties, iron oxides have the potential to be used to treat water contaminated with toxic metals and other contaminants (Omoregie et al., 2013).

Phosphate is often found in waters where iron oxides are present (Weng, Van Riemsdijk & Hiemstra 2012). Phosphorous is the limiting nutrient in most ecosystems, specifically freshwater systems (Glasauer et al., 2003; Zeng, Li & Liu 2004). When it is present in freshwater, enzymes will hydrolyze phosphorous into phosphate, and contributes to the process of eutrophication (Correll 1999). Eutrophication is a widespread problem in bodies of water, particularly fresh water because of what it produces (Correll 1999 and Weng et al., 2012). It has detrimental ramifications due to the production of algal blooms, harmful cyanobacteria and other microorganisms, unwanted odours and it can also be detrimental to fish (Weng et al., 2012). The detailed processes of eutrophication and its products will not be discussed, however it is important to recognize that iron oxides can assist in minimizing the detrimental effects of eutrophication because phosphate in solution has a high affinity for iron oxide surfaces, and they are able to adsorb it and remove it from solution (Cornell & Schwertmann 2003; Glasauer et al., 2003).

A stable and efficient method to removing phosphorous contaminants in secondary effluent is through adsorption onto iron oxides (Kang et al., 2003). These authors investigated the percentage of phosphate adsorption onto three different iron oxides, one of them being ferrihydrite, from wastewater samples. The results showed that ferrihydrite among the three iron oxides studied provided the highest percentage of phosphorous removal (60%), and increasing concentrations of the iron oxide were attributed to higher percentage of P removal. This is due to the fact that ferrihydrite has a high surface area of approximately 200 to 300 m^2/gram (Kang et al., 2003). Another study conducted by Rhonton and Bigham (2005) investigated the removal of phosphorous from seven different soil samples doped with ferrihydrite. The ferrihydrite was collected from a water treatment plant in the form of a sludge by-product. Different amounts ranging from 0.15-15 g ferrihydrite/kg soil were applied to determine the final concentration of phosphorous, thus revealing how much was adsorbed onto the ferrihydrite. The results for each soil sample showed that phosphorous concentrations were minimized, decreasing by approximately at least 50%, and the variation was due mainly to soil pH (Rhonton & Bigham 2005).

However, microbial reactions play a large role in iron cycling which in return affects the compounds, ions and metals that iron oxides help regulate (Gault et al., 2011). There is a sizeable amount of iron in both anoxic soils and sediments, and Fe(III) usually takes the main role of being an electron acceptor in these locations (Kappler & Straub 2005). When there are iron-reducing bacteria, they facilitate the reduction of Fe(III) to Fe(II), which generates soluble Fe(II) (Fortin & Langley 2005). Biogenic iron oxides (BIOS) are a specific type of iron oxides that form in close association with bacteria

(Châtellier , Fortin, Leppard, & Ferris 2001; Fortin & Langley 2005), especially when the O_2 partial pressure is low (Langley et al., 2009). Natural BIOS have been shown to be reduced in the natural environment, creating a tight oxidation-reduction loop in sediments and also altering the local geochemistry (Gault et al., 2011). Research by Langley et al., (2009a) demonstrated that BIOS are efficient sorbents. This is because they contain hydrous ferric oxide and exopolysaccharides that both have sorption sites for soluble contaminants. However, microbial reduction can alter the stability of the BIOS and can cause the sorbed contaminants to return into solution. Their stability is therefore important for the removal of contaminants.

Alterations of iron oxides, such as ferrihydrite, that occur from reduction reactions caused by iron-reducing bacteria have a prominent impact on where and how contaminants and/or nutrients, such as phosphate, end up (Borch et al., 2007). The type of microorganisms which can initiate and perform the reduction from Fe(III) to Fe(II) are dissimilatory iron-reducing bacteria (DIRB) (Borch et al., 2007; Salas et al., 2010).

The present study investigates the redox stability of synthetic BIOS that has phosphate incorporated into its structure, simulating iron oxides present in wastewater treatments using BIOS to remove phosphorous. Specifically, does the presence of phosphate within the structure of the iron oxides make them less reducible than synthetic pure ferrihydrite? Experiments will be to done to explicitly address whether or not the addition of phosphate (PO_4) will alter the formation of ferrihydrite, and thus its interaction with *Shewanella putrefaciens* CN32 and its iron reducing capabilities. Results will be compared to pure synthetic ferrihydrite as well as ferrihydrite and alginate, which was conducted under identical conditions. *Shewanella putrefaciens* CN32 is a facultative

anaerobe dissimilatory iron-reducing bacterium (DIRB) that has a fast generation time (Glasauer, Langley & Beveridge 2002; Borch et al., 2007). *S. putrefaciens* uses Fe(III) as its electron acceptor during the electron transport chain process of the oxidation of lactate and/or acetate in order to generate energy (Borch et al., 2007). Based on the work of Châtellier et al., (2004), it is hypothesized that phosphate will stabilize the ferrihydrite in BIOS, and therefore lower the microbial reduction rate when compared to that of pure ferrihydrite BIOS.

Materials and Methods

Ferrihydrite Synthesis

Synthesis of 2-line ferrihydrite was conducted by combining the modified methods of Mikutta et al., (2008) and Schwertmann and Cornell (2000). One litre beakers and stir bars were autoclaved for sterilization purposes and 550 mL of Millipore water was added to them and placed on a stir plate. 4.04 grams of ferric nitrate in the form of $Fe(NO_3)_3 \cdot 9H_2O$ was added. 1M NaOH was slowly added (approximately 28 mL in total) to help the solution attain a pH of 7.0. The solution was then left to settle to separate the water from the precipitate. Water was removed and the remaining sample of ferrihydrite was combined into centrifuge tubes, approximately 32 tubes with 30 mL of volume in each. The ferrihydrite suspension was centrifuged at 3000 rpm for 15 minutes and washed four times with Millipore water and stored in the fridge.

Ferrihydrite + Alginate Synthesis

Another set of samples was prepared with alginate in order to synthesize a mixture of ferrihydrite and polysaccharides resembling natural BIOS. Alginate simulates

exopolysaccharides (sugars) being present in BIOS. 0.5 grams of alginate was added to 500mL of Millipore water and left for 24 hours to dissolve using a stir bar and a stir plate. The pH of the solution was brought to 2.5 by addition of 1M HNO_3 (between 2 and 2.6 mL were added based on several trials). Ferric nitrate (4.04 g) was then dissolved in 50 mL of Millipore water and added to the alginate solution. The remaining steps to adjust pH were the same as in the ferrihydrite synthesis.

Addition of Phosphate

Samples with phosphate were prepared the same way as above, however when adding phosphate to the ferrihydrite + alginate, NaH_2PO_4 was added prior to the addition of ferric nitrate. A solution of 1 uM NaH_2PO_4 was added to the ferrihydrite solutions with and without alginate. The volume added was 66uL and the calculation is outlined in equation 1 the appendix.

Phosphate Content

Acid digestion was conducted to determine the actual amount of phosphorous that was incorporated in the four different ferrihydrite samples during synthesis, i.e., ferrihydrite, ferrihydrite + alginate, ferrihydrite + PO_4 and ferrihydrite + alginate + PO_4. Two digestion trials were performed for each sample. Approximately 0.5 grams of each sample was weighed out into a vial, 6 mL of deionized water added, 4 mL of hydrogen peroxide (H_2O_2) and lastly 2mL of nitric acid (HNO_3). The samples were left to sit in the fume hood for 24 hours, then moved to an oven at 70 degrees Celsius to sit for another 24 hours. The samples were then sent off for iron and phosphorous analysis by inductively-coupled plasma atomic emission spectroscopy (ICP-AES).

Iron content

A dithionite extraction as outlined by methods in Kostka and Luther (1994) was performed to determine the total iron content (i.e., amorphous and crystalline) of the various samples. Approximately 0.02 grams of sample was weighed and 10 mL of a solution containing 2 mL of glacial acetic acid, 98 mL of water and 5.882 grams of sodium citrate dehydrate were added. The suspension was placed in oven at 70 degrees Celsius for 1 hour. 0.5 grams of dithionite powder was then added and the suspension was returned to the oven for 1 hour. Vials were then cooled, and 100 uL of sample was added to 5mL of ferrozine solution (1 g of ferrozine and 12 g of HEPES buffer were added to 1L of water). The pH was adjusted to 7.0 with NaOH as needed and placed in darkness for 30 minutes. The absorbance of each final solution was measured at 562 nanometers, and this value was used to calculate the final mass of iron oxide to be used. The average mass of all three trials was taken as the mass of iron oxides to be added for reductions as calculated in the appendix.

X-ray Diffraction

Mineralogy of the different ferrihydrite samples was determined using powder X-ray diffraction analysis. Samples were dried in a fume hood for approximately 48 hours and then ground into a fine powder using a mortar and pestle (Langley et al., 2009). Samples were sent off for analysis using a Rigaku X-ray diffractometer with a scan range from 5 to 80 degrees (2 theta) at a step scan size of 0.02 degrees.

Shewanella putrefaciens CN32 Growth

S. putrefaciens CN32 was maintained on a tryptic soy agar plate at room temperature. A colony was grown in 50 mL of tryptic soy broth (TSB) on a rotary shaker at 150 rpm. After 24 hours 1 mL of the TSB culture was placed into 50 mL of a sterile 50:50 CDM:TSB mixture, which was incubated at 150 rpm for 24 hours. This was repeated with mixtures of 95:5 and 99:1 CDM:TSB, with 190 and 198 μL of phosphate, respectively. After 24 hours 4 mL of the 99:1 mixture was sub-cultured into 100 mL of CDM with 400 μL of phosphate and incubated for 48 hours. The cells were harvested by centrifugation (15 minutes at 3000 rpm) and suspended in a small amount of fresh CDM, approximately 2mL.

Microbial Reduction Microcosms

A chemically defined medium was prepared for the reduction microcosms. 1.5 grams of 1,4-piperazinediethanesulfonic acid (PIPES) buffer, 3.75 grams of sodium lactate, 10mL of a trace metal solution and 10mL of a stock solution were added to1 L of Millipore water and then autoclaved (Langley et al., 2009). This was done in order to prepare enough volume to have four 1L bottles filled with 700 mL of CDM. The microcosms were prepared in the 4 sterile 1L bottles that the CDM were prepared in. 2.73 mL of 1M phosphate was added to each bottle, and the pH adjusted to 7.0 using 8M NaOH and 6M HCl as needed. The determined amount of ferrihydrite sample was added (equivalent to 4 mM of Fe). This includes 3 trials of each ferrihydrite sample and a control system whereby no bacterial cells were added to the medium containing the various ferrihydrite samples. Once the bottles were in the anaerobic chamber, the pre-determined inoculum of *S. putrefaciens* CN32 as calculated in equation 2(see appendix)

was added to Trials 1-3, and none to the control in order to compare biotic and abiotic reductions. The following sampling procedures were done every two days, approximately 48 hours apart. Immediately after the addition of the cells, the bottles were shaken and approximately 20 mL poured out into a scintillation vial to sample from. Sub-samples were taken for cell counts, total iron (Fe(II) + Fe(III)), dissolved Fe(II) and total dissolved Fe, pH and redox measurements. For the dissolved measurements, the samples were filtered with a 0.22 um acro-disk attached to a syringe. The iron concentration was determined with the ferrozine method as outlined by Stookey (1970). To determine the dissolved iron amounts, 0.5 mL of filtered sample was added to 4.5 mL of 0.5 M HCl and to determine total iron 0.5 mL of sample from the scintillation vial was added to 4.5 mL of 0.5M HCl. The samples were stored in the anaerobic chamber for 24 hours. After 24 hours, the samples were removed from the chamber and vortexed. The following procedures were conducted twice, first with the dissolved sample and then with the total sample. To determine the Fe(II) content, 900uL of ferrozine was added to 20uL of acidified sample (dissolved or total) and the solutions were left to stand for 10 minutes, using ferrozine as the blank. For the total iron content, 100 uL of the acidified sample was added to 900 uL of hydroxylamine and HEPES buffer solution (0.2 grams of hydroxylamine, 1.2 grams HEPES. buffer and 100 mL Millipore water) and left to stand for 20 minutes. Immediately after, 100 uL of this solution was transferred into 900 uL of ferrozine, with hydroxylamine and HEPES buffer as the blank and left again to stand for 10 minutes. The total absorbance was then read at 562 nM using an ultrospec 1100 pro spectrophotometer. Absorbances were converted to mM of iron using a ferrozine calibration curve to determine the equation (figure 11 and 12 in appendix). A rate of

reduction as a molar ratio of Fe(II)/Fe(III) per day was calculated to determine the speed of iron reduction. A welch two-sample T-test was conducted using the statistical software R version 3.2.1 to compare the rates of reductions The number of cells was determined with the most-probable-number method using TSA agar plates. The average cell counts at each sample time from Trials 1,2 and 3 were taken for dilutions of 10^{-4}, 10^{-5} and 10^{-6}, converted to colony forming units per millilitre (CFU/mL) (equation 5 in appendix), and then an overall sample time average in CFU/mL was plotted.

Results

Mineralogy and chemical composition of the various ferrihydrite samples

X-ray Diffraction

The X-ray diffraction patterns displayed in Figure 1 of all four samples had peaks that are consistent with ferrihydrite XRD standards.

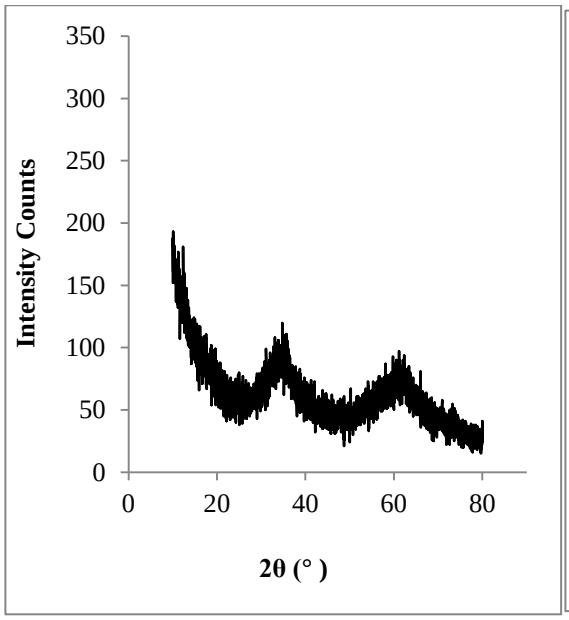

A) Ferrihydrite

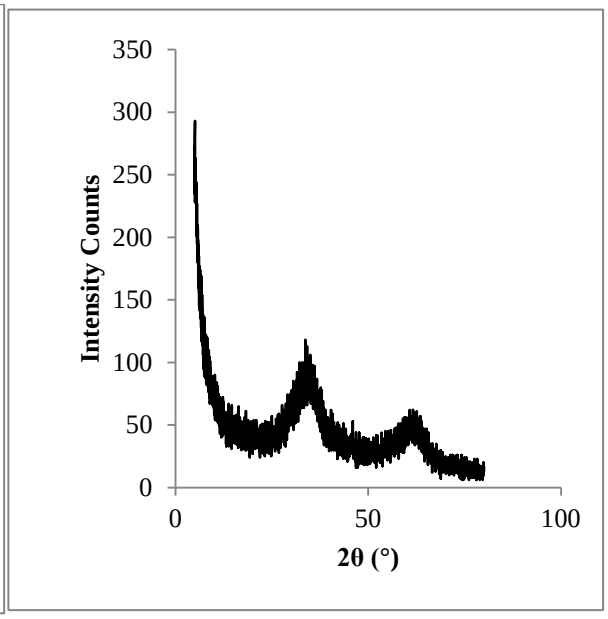

B) Ferrihydrite + PO_4

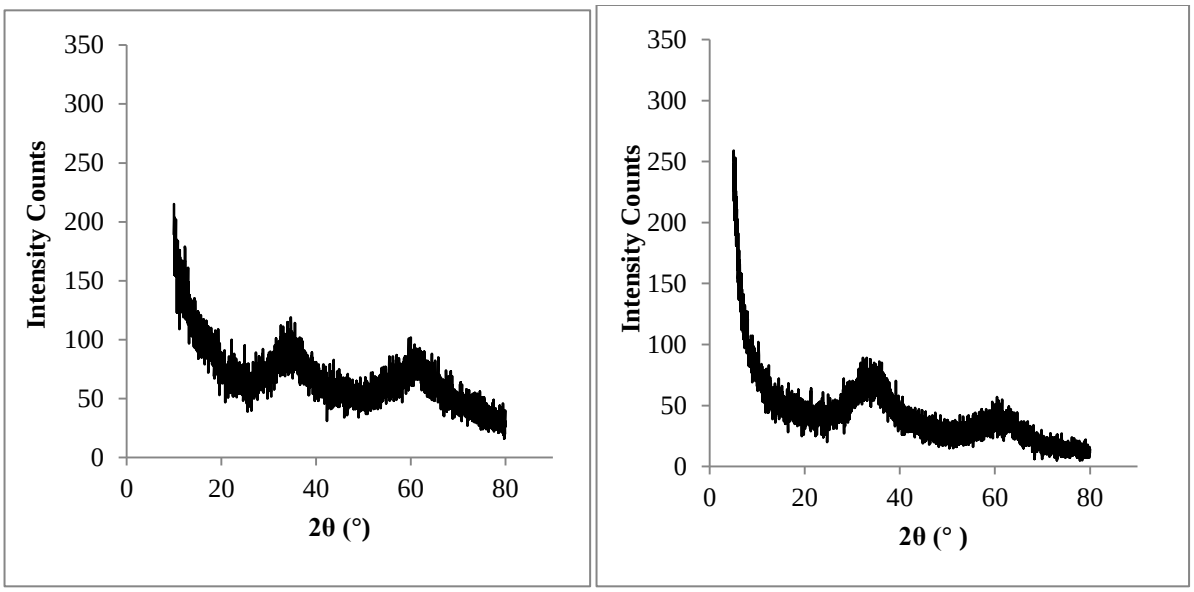

C) Ferrihydrite + Alginate D) Ferrihydrite + Alginate + PO_4

Figure 1: XRD of A) Ferrihydrite B) Ferrihydrite + PO_4 C) Ferrihydrite + Alginate D) Ferrihydrite + Alginate + PO_4

Phosphate Content

As noted in Table 1, the pure ferrihydrite samples had no phosphate and the sample with alginate and PO_4 added had the highest ratio. The results also indicate that alginate is a source of phosphate.

Table 1: Phosphorous content of the various ferrihydrite samples

Sample	**P to Fe as a Molar Ratio**
Fh Trial 1	0
Fh Trial 2	0
Fh + PO_4 Trial 1	0.0042

Fh + PO_4 Trial 2	0.0043
Fh + Alginate Trial 1	0.0097
Fh + Alginate Trial 2	0.0110
Fh + Alginate+ PO_4 Trial 1	0.0118
Fh + Alginate+ PO_4 Trial 2	0.0122

Reduction microcosms

Prior to the microbial reduction, the microcosms had a homogeneous dark rusty red colour throughout (Figure 2 A and C). At the end of the reduction, the bottles were not homogeneous in colour as there was distinct separation of sediment at the bottom of the bottle from the solution (Figure 2 B and D). The solutions became much more transparent in colour, specifically Trial 1 of ferrihydrite + PO_4 reduction.

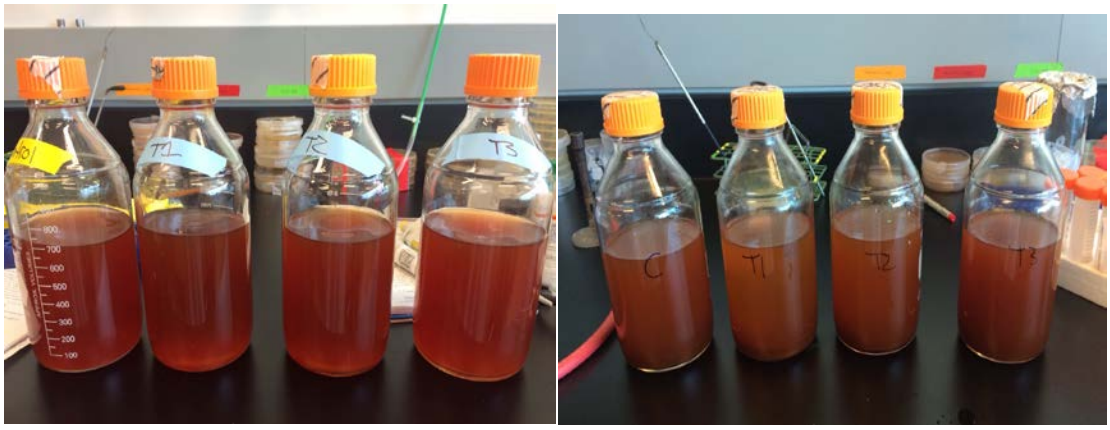

A) B)

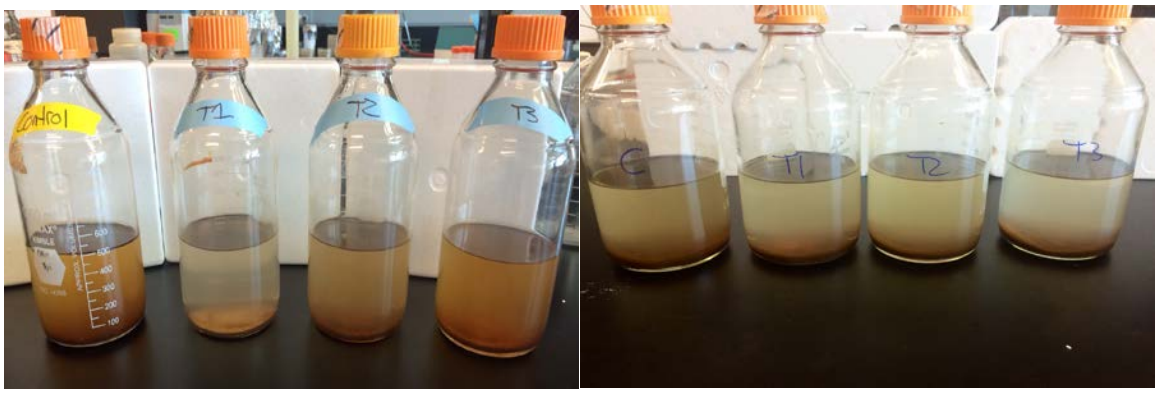

C) D)

Figure 2: Reduction microcosm bottles at T0, A) Ferrihydrite + PO_4, B) Ferrihydrite + Alginate + PO_4. Reduction microcosm bottles after the reduction C) Ferrihydrite + PO_4 at sample time T10 D) Ferrihydrite + Alginate + PO_4 after sample time T9

pH Results

The pH as shown in Figures 3 and 4 in all microcosms remained fairly stable over the reduction period hovering at about a pH of 7. The variation was low, remaining between 6.60 and 7.40. The pH of the trial experiments tended to vary more in all trials except for the ferrihydrite + alginate + PO_4 sample. The ferrihydrite sample and its control continued to remain above 7.00, hovering towards the high end of the range. The ferrihydrite + PO_4 + alginate samples had the most drastic decrease from its starting pH and began to stabilize at a slightly acidic pH around day 10 where the readings hovered among the lower end of the pH range. The experiments without PO_4 added had pH values which varied less than when PO_4 was added. Specifically, they did not follow a general trend of having as much of a decrease as the samples with phosphate. The pH of the experiment with ferrihydrite + PO_4 added experienced a significant decrease, and then increased again towards the peak of the reduction. The control followed a similar trend, at a later date. The control and trials followed the same trend at approximately the same

time and this may be due to the control being contaminated, as illustrated in the cell count results.

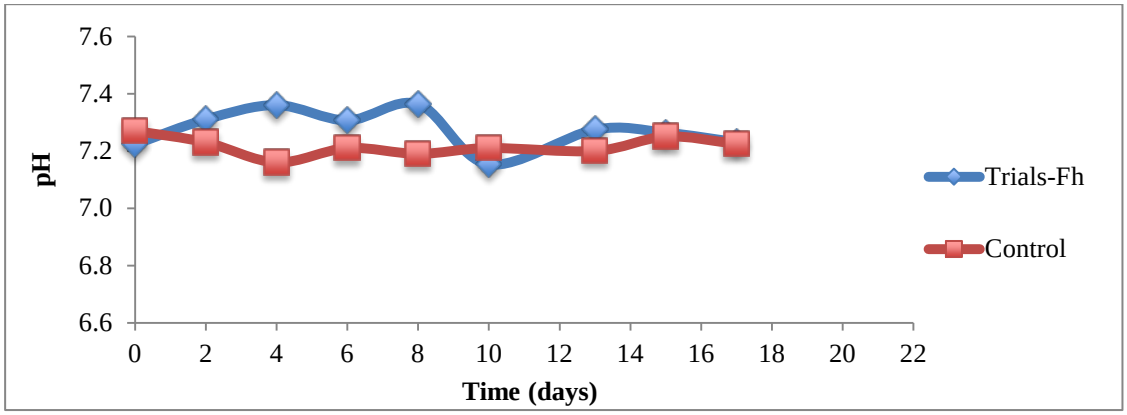

A)

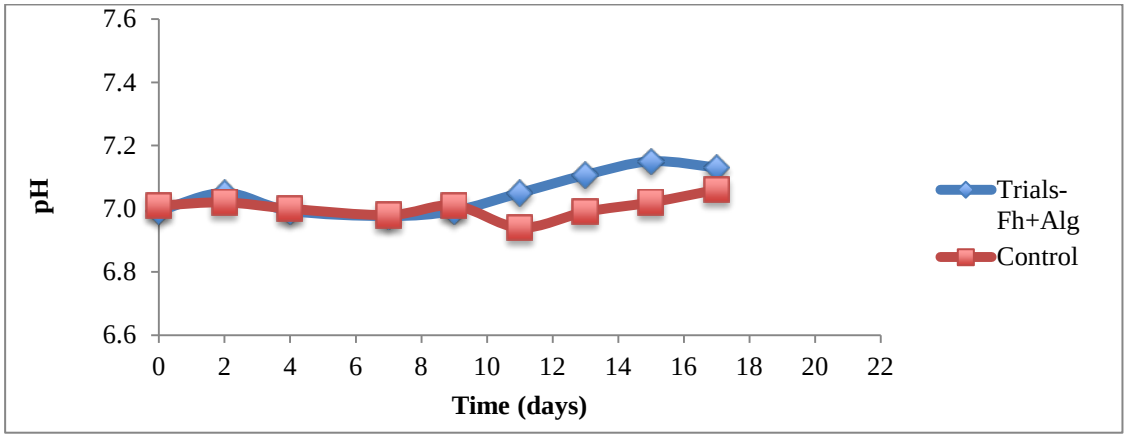

B)

Figure 3: Average pH values of the microcosms without phosphate A) ferrihydrite B) ferrihydrite + Alginate

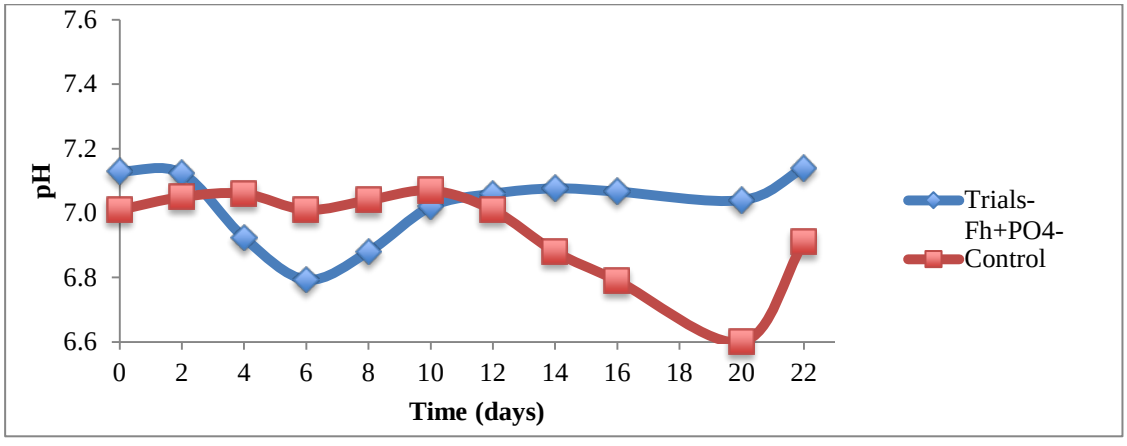

A)

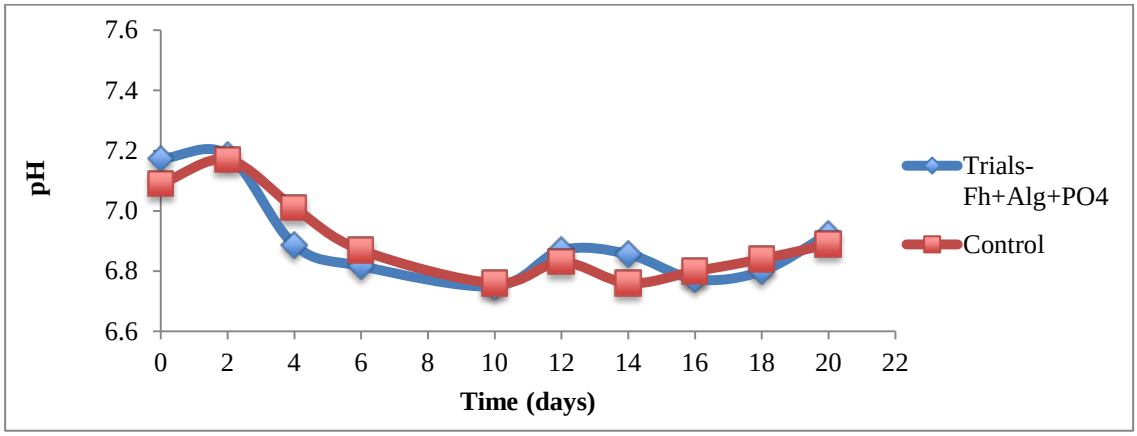

B)

Figure 4: Average pH values of the microcosms with phosphate A) ferrihydrite + PO_4 and B) ferrihydrite + Alginate + PO_4

Eh results

In all four biotic microcosms, reducing conditions developed during the course of the reduction, as shown by the decreasing redox values overtime (Figure 5). The Eh values levelled off at about -150 millivolts. Redox values remained constant overtime in the control systems, with the exception of both the ferrihydrite + PO_4 and ferrihydrite + alginate+ PO_4 samples, where reducing conditions developed overtime (Figures 5C and D). These results suggest that these control systems became contaminated with *S. putrefaciens* cells during sampling.

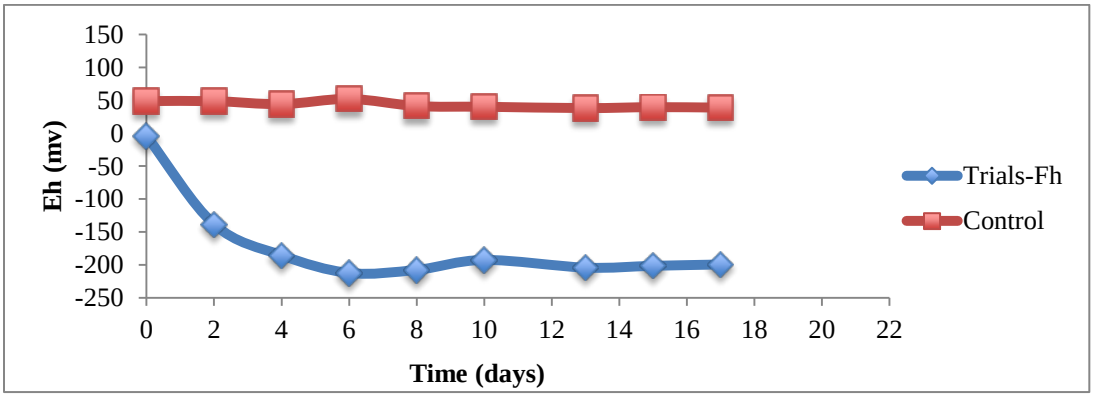

A)

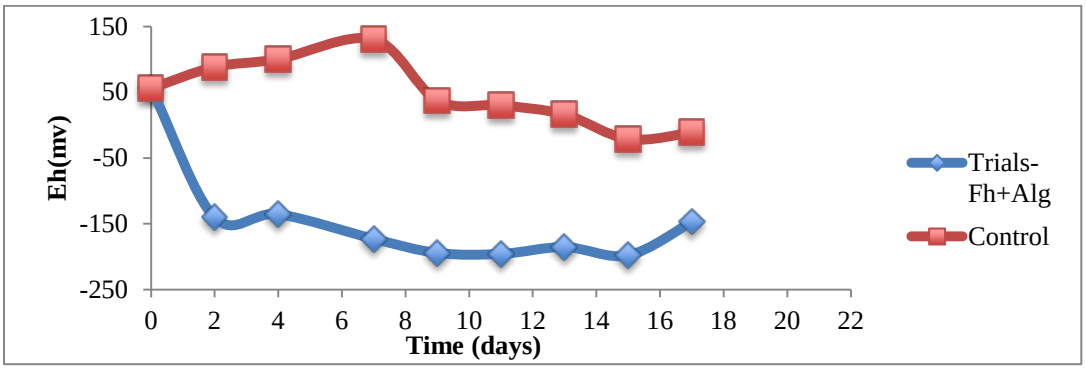

B)

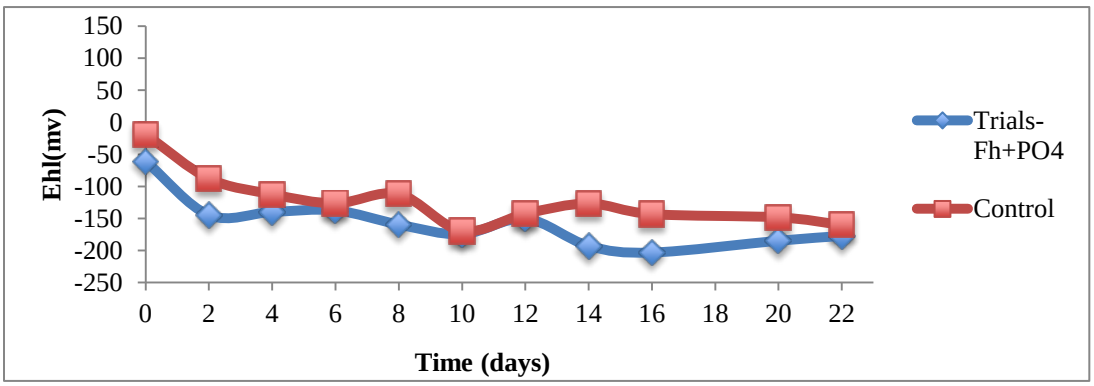

C)

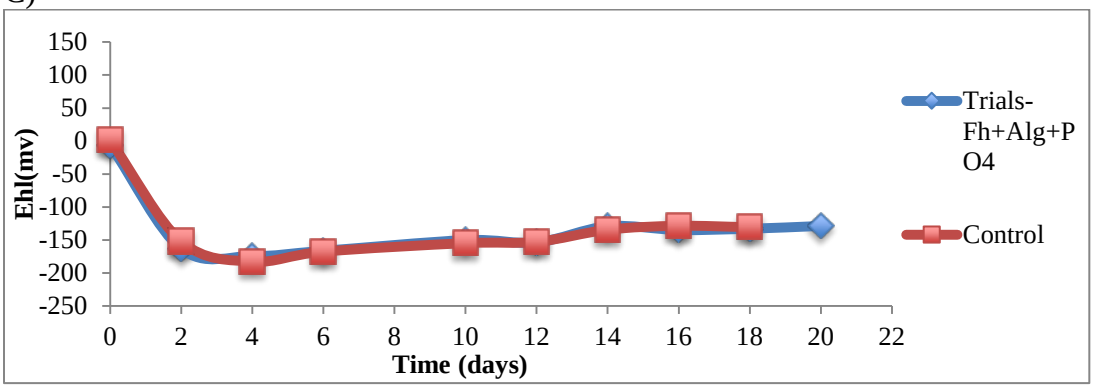

D)

Figure 5: Average Eh values of the microcosm containing A) ferrihydrite B) ferrihydrite + Alginate C) ferrihydrite + PO_4 and D) ferrihydrite + Alginate + PO_4

Microbial reduction

The process to determine the Fe(II) to Fe(III) ratio is outlined in the appendix. The onset of iron reduction (expressed as a percentage of Fe(II) total over Fe total) in all biotic systems started slowly in the first week (Figures 6-9). In the second week, the

range increased, ranging from 20% to 100%, depending on the microcosm. The highest Fe(II)/Fe total ratio was observed in the ferrihydrite alone and ferrihydrite + alginate systems (Figures 6 and 7). The samples containing PO_4 attained a slightly lower percentage of iron reduction as shown in Figures 8 and 9. All trials within each sample followed a very close trend and all reached their peak of reduction after two weeks. The control systems showed lower Fe(II)/Fe total ratios than the biotic ones. The calculated rates of reduction are shown in Table 2. The rates were low over all due to an apparent delay of active reduction in the first week. The highest rates was observed in the ferrihydrite + alginate system whereas the lowest one was measured in the ferrihydrite +alginate+ PO_4 system. The fastest microcosm reduced approximately 18% more Fe(III) per day compared to the slowest one.

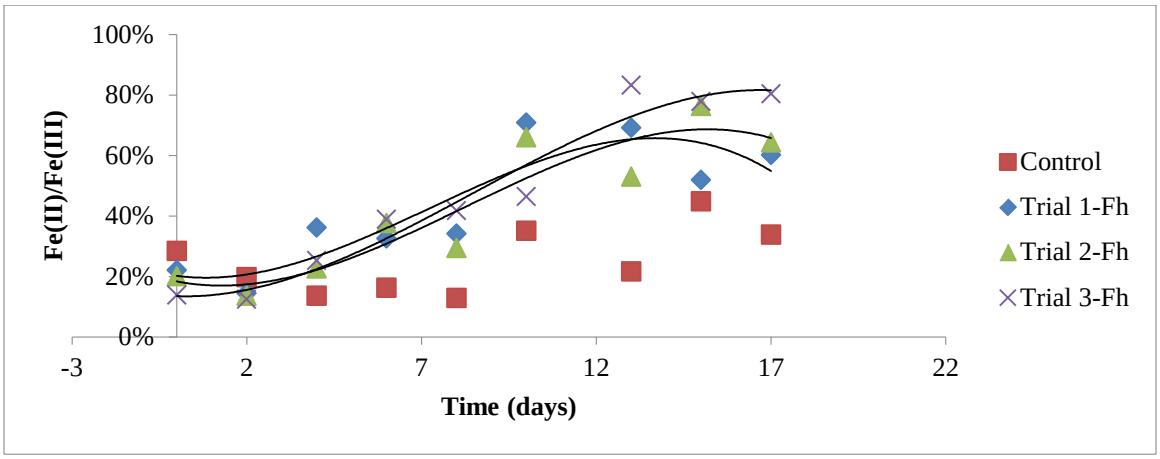

Figure 6: Fe(II)/Fe molar ratio (displayed as %) during the course of the reduction of Ferrihydrite.

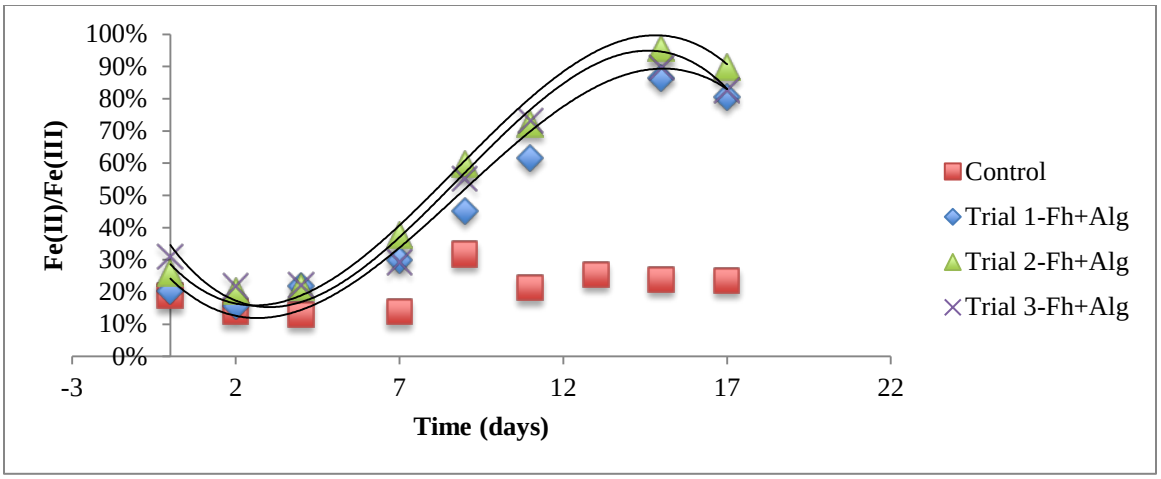

Figure 7: Fe(II)/Fe molar ratio (displayed as %) during the course of the reduction of Ferrihydrite + Alginate.

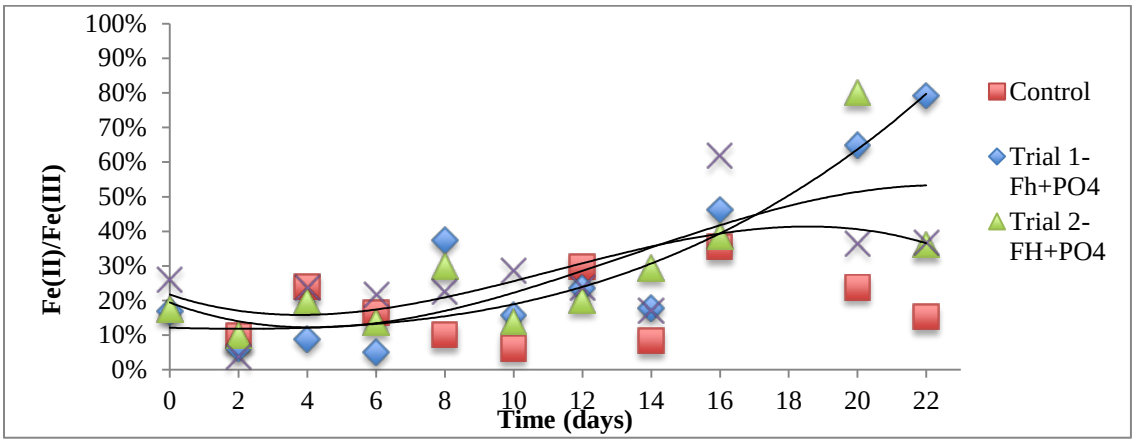

Figure 8: Fe(II)/Fe molar ratio (displayed as %) during the course of the reduction of Ferrihydrite + PO_4

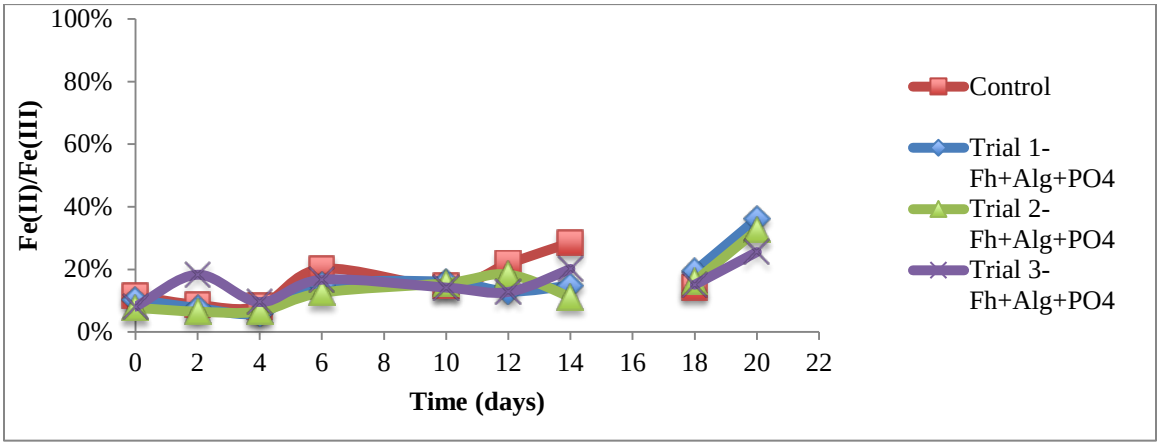

Figure 9: Fe(II)/Fe molar ratio (displayed as %) during the course of the reduction of Ferrihydrite + Alginate + PO_4

Rates of Reduction

Table 2: Rates of reduction of the various samples (Figures 6, 7, 8 and 9). Calculations are in the appendix in Table 7.

Sample	**Average Rate (mM Fe(II)/ Day)**	**Standard Deviation**
Ferrihydrite	0.0611	0.0115
Ferrihydrite + PO_4	0.0423	0.0038
Ferrihydrite +Alginate	0.0774	0.00316
Ferrihydrite +Alginate+ PO_4	0.0141	0.0049

Statistical Test on Rate of Reductions

The average rate of reduction of ferrihydrite was not statistically different from that of ferrihydrite + alginate or ferrihydrite + PO_4, but was different from that of ferrihydrite + alginate + PO_4 (Table 3). The results for the ferrihydrite + alginate system were statistically different from those of ferrihydrite + PO_4. The rate for ferrihydrite + alginate + PO_4 was statistically different from that of ferrihydrite + alginate and ferrihydrite + PO_4.

Table 3: Rates of reduction T-Test Results at a 95% Confidence Interval *$p<0.05$

Sample 1	**Sample 2**	**P Value**
Ferrihydrite	Ferrihydrite + Alginate	0.1253
Ferrihydrite	Ferrihydrite + PO_4	0.09345

Ferrihydrite	Ferrihydrite + Alginate + PO_4	0.01003
Ferrihydrite + PO_4	Ferrihydrite + Alginate	0.0003018
Ferrihydrite + PO_4	Ferrihydrite + Alginate + PO_4	0.001839
Ferrihydrite + Alginate	Ferrihydrite + Alginate + PO_4	0.0001481

Cell count results

For all biotic systems, the number of cells declined over of the course of the experiment (Figure 10). All systems contained 10^7-10^8 CFU/mL at the beginning of the experiment. Cell counting using agar plates showed that the ferrihydrite + alginate + PO_4 control(abiotic) microcosm was contaminated throughout, the colonies present were distinctly different than those of *S. putrefaciens*. The contamination source is unknown.

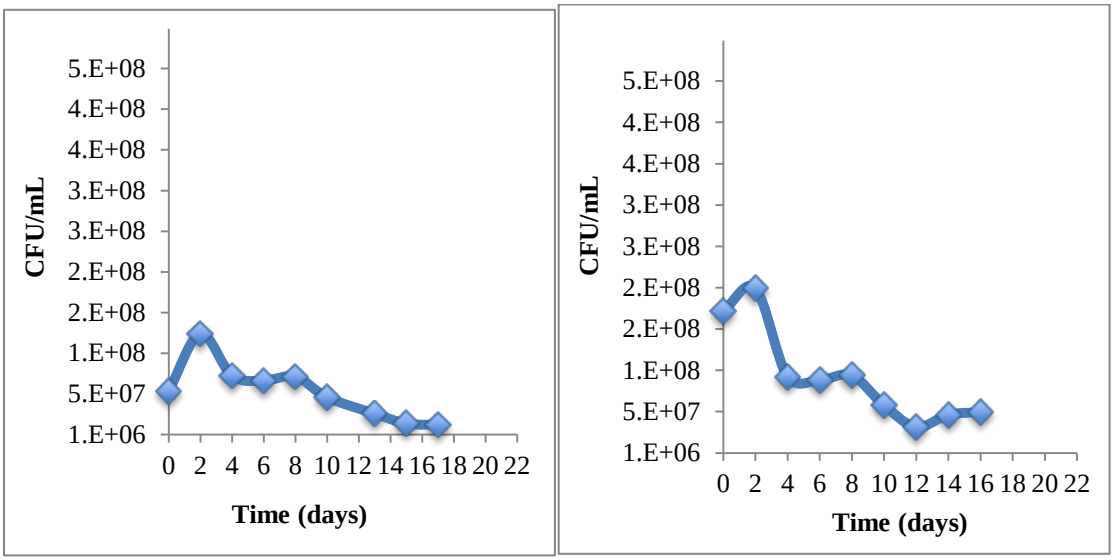

A) B)

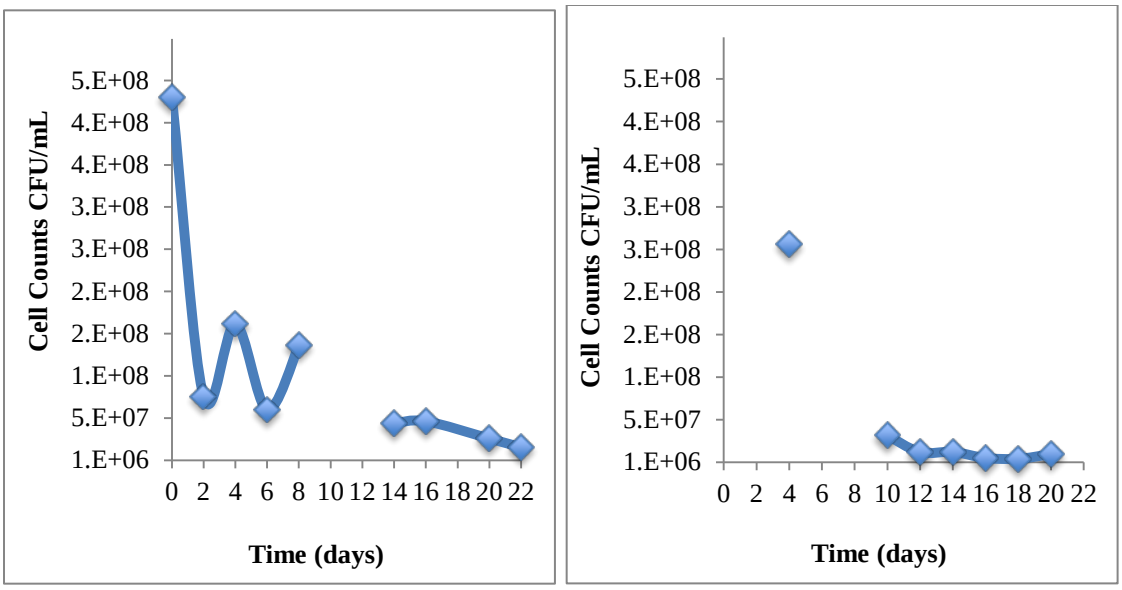

C) D)

Figure 10: Average cell counts in CFU/mL of A)Ferrihydrite B) Ferrihydrite + Alginate C)Ferrihydrite + PO_4 and D) Ferrihydrite + Alginate + PO_4. (There are missing data for the microcosm with ferrihydrite + PO_4 at times T5 and T6 and ferrihydrite + alginate + PO_4 at times T0, T1 and T3 because of a human error.)

Discussion

Mineralogy and chemical composition of the various ferrihydrite samples

The addition of phosphate and/or alginate during the synthesis of ferrihydrite did not affect its mineralogy. The two main diffraction peaks in all four samples (Figure 1) are at approximately 35 and 60 degrees. These correspond to previous XRD results of 2-line ferrihydrite synthesized in the presence of alginate (Kukkadapu, et al., 2004; Mikutta et al., 2008).

The ICP results (Table 1) indicated that the ferrihydrite + alginate + PO_4 sample contained the highest amount of phosphorous. This is explained by the fact that alginate contains phosphorous, which was determined to be 114ug/g (Mikutta et al., 2008). This also means that the ferrihydrite + alginate sample contains phosphate, in the form of structural P in alginate, but not sorbed or incorporated into the iron oxides. The

implications of this are that upon microbial reduction, only the phosphate associated with the ferrihydrite will be released into solution, not the structural P.

Microbial Reductions

Our results showed that *S. putrefaciens* was capable of reducing all ferrihydrite samples as evidenced by the increasing Fe(II)/Fe total ratios overtime (Figures 6-9). This was accompanied by the development of reducing conditions in the biotic systems (Figure 5). The biotic systems also changed colour overtime as displayed in Figure 2 with the formation of secondary Fe(II)-rich minerals, as also observed in previous studies with the same strain (Glasauer et al., 2003; Langley et al., 2009). Interestingly, the cells did not grow during the reduction (Figure 10), in fact they started to decline shortly after the inoculation. The lack of growth was attributed to the stationary growth phase and beyond whereby cells start to die at the same rate as they grow, eventually dying at a faster rate than growing (Glasauer et al., 2003). During the course of the reduction, the pH remained fairly constant, but decreased slightly in some systems as a result of proton translocation (Lovely 1993). The equation below outlines the reaction that occurs when the oxidation of lactate is coupled to the reduction of Fe(III).

$$lactate^- + 4Fe(III) + 2H_20 \rightarrow acetate + HCO_3^- + 4\ Fe(II) + 5H^+$$

Lactate was added to the microcosms in the form of sodium lactate. When this reaction occurs, hydrogen ions are released, which explains why the pH slightly dropped throughout the reduction in some systems. The pH varied approximately within the same upper and lower limits as in the study by Glasauer et al., (2003). Since not all microcosms behaved exactly the same, it is likely that other reactions (such as secondary mineral formation) contributed to the observed pH changes.

Langley et al., (2009) reported that with synthetic ferrihydrite, maximum percent of total ferric iron reduced was 78.08% +/- 0.68. This is significantly higher than what was previously reported when ferrihydrite samples with added phosphate (i.e., maximum reduction values between 40% and 60% at the peak of the reduction) (Glasauer et al., 2002; Glasauer et al., 2003). These values however align with the results from this study with the system containing ferrihydrite + PO_4 (Figure 7). Our results show that the presence of phosphate (bound or incorporated into the ferrihydrite, not phosphate from alginate) lowered the microbial reduction rate (Table 2). Kukkadupa et al., (2004) demonstrated that increasing phosphorous concentrations in ferrihydrite decreased the Fe(II)/Fe(III) ratio during reduction with *S. putrefaciens* CN32, which supports the fact that phosphate stabilizes ferrihydrite. The results from Borch et al., (2007) also provide support to our results. Their study, which varied phosphate coverage over iron oxide samples with *S. putrefaciens*, demonstrated that as the phosphate coverage increased, Fe(II) decreased (Borch et al., 2007). This is due to the fact that phosphate stabilizes the Fe(III)-oxides causing less reduction to occur. The study by Borch et al., (2007) had 13% of the synthetic ferrihydrite with 4 mM PO_4 reduced at 39 days, which was similar to the study by Zachara et al., (1998), which demonstrated a 13.4% reduction of ferrihydrite in the presence of 4 mM phosphate after 39 days. The concentration of phosphate within our experiment microcosms was significantly lower than that in the studies by Borch et al. (2007) and Zachara et al. (1998), however it still demonstrates that the presence of phosphate slows down the microbial reduction of ferrihydrite.

Our rates of reduction (Table 2) are somehow comparable to what has been published previously. Glasauer et al., (2003) investigated the effects of varying phosphate

concentrations with different iron oxides. One scenario investigated was with HFO (ferrihydrite) with 4 mM or 0.4 mM phosphate and *S. putrefaciens* CN32. The length of the reduction was 46 days, approximately double to triple the length of our experiment. In the Glasauer et al., study, two of the reduction rates in trials with 4mM phosphate were of similar order of magnitude to our experiments with rates of 0.021/day and 0.036/day (Glasauer et al., 2003). Langley et al., (2009) had rates of reduction for synthetic ferrihydrite at 0.162 Fe(II)/Fe total per day, faster than what is normally reported. Reduction rates reported by Langley et al., (2009) for natural BIOS were between 0.269 and 0.467 per day, which is significantly faster than our rates (Table 2) and other ones reported rates in literature. Studies comparing synthetic and natural BIOS demonstrate that even with the same mineralogy, the natural BIOS will often reduce faster because of additional organic components in natural settings (Langley et al., 2009).

Lastly, it is possible that our reported rates of iron reduction by *S. putrefaciens* CN32 were impacted by small amounts of nitrate in the microcosms. As outlined in the methods, the synthesis of the 4 ferrihydrite samples used ferric nitrate $Fe(NO_3)_3 \cdot 9H_2O$. In addition, HNO_3 was added to the microcosms that had alginate to adjust the pH. In previous studies, such as Glasauer et al., (2002, 2003), Langley et al., (2009) and Zachara et al., (1998), the standard chemical used to synthesize ferrihydrite is ferric chloride in the form of $FeCl_3 \cdot 6H_20$. Using ferric nitrate or chloride will not impact the mineralogy of ferrihydrite, however it may affect the reduction of Fe(III), since nitrate is a preferred electron acceptor over iron. Microorganisms prioritize the use of certain electron acceptors based on redox potential, using acceptors that have the highest redox potential first (Achtnich et al., 1995). These authors showed that the addition of nitrate and ferric

iron to paddy soil samples caused the preferential reduction of nitrate over iron. In addition, *S. putrefaci*ens CN32 is a known nitrate reducer (Qiu et al., 2013). It is therefore highly possible that it reduced the nitrate present in the microcosms, which delayed the onset of ferrihydrite reduction, as indicative by some of our results.

Implications for wastewater treatment

Removal of phosphate through sorption onto biogenic iron oxides (BIOS) has been shown to be a promising water treatment (Rentz et al., 2009). Different types of water sources can be treated with BIOS in order to sorb the contaminants that are present, and this produces a sludge, which contains the contaminants (Paige et al., 1997). The issue that arises with this BIOS treatment is the disposal of the sludge after its use (Paige et al., 1997). The most common method of disposal is to take it to a landfill, however this may pose major issues for water quality nearby. There is the threat of the landfill leaching and seeping into the ground, and this can lead to groundwater contamination, which is often a source of drinking water (Omoregie et al., 2013; Paige et al., 1997). The likelihood of this happening is greatly increased if the BIOS are not stable (Paige et al., 1997). Borch et al., (2007) suggested that the more phosphate and potentially other contaminants present near the iron oxides, the more stable it will make the ferrihydrite. Ensuring the stability of the iron oxides is therefore necessary. As demonstrated in this study, even though phosphate stabilizes ferrihydrite, the ferrihydrite + PO_4 and the ferrihydrite + alginate + PO_4 samples underwent microbial reduction (Figures 8 and 9) and released their sorbed phosphate into solution. A way to avoid potential issues with PO_4-rich BIOS instability is to use the sludge as a fertilizer for agricultural and farming

purposes (Wei, Viadero & Bhojappa 2008). This offers a more sustainable method than disposal to a landfill, because phosphorous is needed for crops to grow. Further research is needed to evaluate the benefits and costs of using BIOS sludge with phosphate as fertilizer compared to disposal into a landfill, but the potential as a sustainable farming practice is promising (Wei et al., 2008).

Conclusion

The experiments done on synthetic ferrihydrite, ferrihydrite with alginate, ferrihydrite with phosphate and a combination of the latter two demonstrate that the addition of phosphate stabilizes the iron oxide and hinders the rate of reduction by *S. putrefaciens* CN32. Further research should however be conducted with ferrihydrite being synthesized using ferric chloride, as it is not an electron acceptor for *S. putrefaciens* CN32 and would thus not interfere with the reduction process. Understanding the stability of biogenic iron oxides is therefore crucial in order to minimize the re-release of sorbed contaminants, such as phosphate, in the environment.

References

Achtnich, C., Bak, F., & Conrad, R. (1995). Competition for electron donors among nitrate reducers, ferric iron reducers, sulfate reducers, and methanogens in anoxic paddy soil. *Biology and Fertility of Soils*, *19*(1), 65-72.

Borch, T., Masue, Y., Kukkadapu, R. K., & Fendorf, S. (2007). Phosphate imposed limitations on biological reduction and alteration of ferrihydrite. *Environmental science & technology*, *41*(1), 166-172.

Châtellier, X., Fortin, D., Leppard, G. G., & Ferris, F. G. (2001). Effect of the presence of bacterial surfaces during the synthesis of Fe oxides by oxidation of ferrous ions. *European Journal of Mineralogy*, *13*(4), 705-714.

Châtellier, X., West, M. M., Rose, J., Fortin, D., Leppard, G. G., & Ferris, F. G. (2004). Characterization of iron-oxides formed by oxidation of ferrous ions in the presence of various bacterial species and inorganic ligands. *Geomicrobiology Journal*, *21*(2), 99-112.

Correll, D. L. (1999). Phosphorus: a rate limiting nutrient in surface waters. *Poultry Science*, *78*(5), 674-682.

Cornell, R. M., & Schwertmann, U. (2003). *The Iron Oxides: Structure, Properties, reactions, Occurences and Uses.* (2nd ed). Weinheim, Germany: Wiley-VCH.

Fortin, D., & Langley, S. (2005). Formation and occurrence of biogenic iron-rich minerals. *Earth-Science Reviews*, *72*(1), 1-19.

Gault, A. G., Ibrahim, A., Langley, S., Renaud, R., Takahashi, Y., Boothman, C., ... & Fortin, D. (2011). Microbial and geochemical features suggest iron redox cycling within bacteriogenic iron oxide-rich sediments. *Chemical Geology*, *281*(1), 41-51.

Glasauer, S., Langley, S., & Beveridge, T. J. (2002). Intracellular iron minerals in a dissimilatory iron-reducing bacterium. *Science*, *295*(5552), 117-119.

Glasauer, S., Weidler, P. G., Langley, S., & Beveridge, T. J. (2003). Controls on Fe reduction and mineral formation by a subsurface bacterium. *Geochimica et Cosmochimica Acta*, *67*(7), 1277-1288.

Kang, S. K., Choo, K. H., & Lim, K. H. (2003). Use of iron oxide particles as adsorbents to enhance phosphorus removal from secondary wastewater effluent. *Separation science and technology*, *38*(15), 3853-3874.

Kappler, A., & Straub, K. L. (2005). Geomicrobiological cycling of iron. *Reviews in Mineralogy and Geochemistry*, *59*(1), 85-108.

Kostka, J. E., & Luther, G. W. (1994). Partitioning and speciation of solid phase iron in saltmarsh sediments. *Geochimica et Cosmochimica Acta*, *58*(7), 1701-1710.

Kukkadapu, R. K., Zachara, J. M., Fredrickson, J. K., & Kennedy, D. W. (2004). Biotransformation of two-line silica-ferrihydrite by a dissimilatory Fe (III)-reducing bacterium: formation of carbonate green rust in the presence of phosphate. *Geochimica et Cosmochimica Acta*, *68*(13), 2799-2814.

Langley, S., Gault, A., Ibrahim, A., Renaud, R., Fortin, D., Clark, I. D., & Ferris, F. G. (2009). A comparison of the rates of Fe (III) reduction in synthetic and bacteriogenic iron oxides by Shewanella putrefaciens CN32. *Geomicrobiology Journal*, *26*(2), 57-70.

Lovley, D. R. (1993). Dissimilatory metal reduction. *Annual Reviews in Microbiology*, *47*(1), 263-290.

Mikutta, C., Mikutta, R., Bonneville, S., Wagner, F., Voegelin, A., Christl, I., & Kretzschmar, R. (2008). Synthetic coprecipitates of exopolysaccharides and ferrihydrite. Part I: Characterization. *Geochimica et cosmochimica acta*, *72*(4), 1111-1127.

Omoregie, E. O., Couture, R. M., Van Cappellen, P., Corkhill, C. L., Charnock, J. M., Polya, D. A., ... & Lloyd, J. R. (2013). Arsenic bioremediation by biogenic iron oxides and sulfides. *Applied and environmental microbiology*, *79*(14), 4325-4335.

Paige, C. R., Snodgrass, W. J., Nicholson, R. V., Scharer, J. M., & He, Q. H. (1997). The effect of phosphate on the transformation of ferrihydrite into crystalline products in alkaline media. *Water, Air, and Soil Pollution*, *97*(3-4), 397-412.

Qiu, D., Wei, H., Tu, Q., Yang, Y., Xie, M., Chen, J., ... & Zhou, J. (2013). Combined genomics and experimental analyses of respiratory characteristics of Shewanella putrefaciens W3-18-1. *Applied and environmental microbiology*, *79*(17), 5250-5257.

Rentz, J. A., Turner, I. P., & Ullman, J. L. (2009). Removal of phosphorus from solution using biogenic iron oxides. *Water research*, *43*(7), 2029-2035.

Rhoton, F. E., & Bigham, J. M. (2005). Phosphate adsorption by ferrihydrite-amended soils. *Journal of environmental quality*, *34*(3), 890-896.

Salas, E. C., Berelson, W. M., Hammond, D. E., Kampf, A. R., & Nealson, K. H. (2010). The impact of bacterial strain on the products of dissimilatory iron reduction. *Geochimica et cosmochimica acta*, *74*(2), 574-583.

Schwertmann, U., & Cornell, R.M. (2000) *Iron Oxides in the Laboratory: Preparation and Characterization*. (2nd ed). Weinheim, Germany: Wiley-VCH.

Stookey, L. L. (1970). Ferrozine---a new spectrophotometric reagent for iron. *Analytical chemistry*, *42*(7), 779-781.

Wei, X., Viadero, R. C., & Bhojappa, S. (2008). Phosphorus removal by acid mine drainage sludge from secondary effluents of municipal wastewater treatment plants. *Water Research*, *42*(13), 3275-3284.

Weng, L., Van Riemsdijk, W. H., & Hiemstra, T. (2012). Factors controlling phosphate interaction with iron oxides. *Journal of environmental quality*, *41*(3), 628-635.

Zachara, J. M., Fredrickson, J. K., Li, S. M., Kennedy, D. W., Smith, S. C., & Gassman, P. L. (1998). Bacterial reduction of crystalline Fe^ 3^+ oxides in single phase suspensions and subsurface materials. *American Mineralogist*, *83*, 1426-1443.

Zeng, L., Li, X., & Liu, J. (2004). Adsorptive removal of phosphate from aqueous solutions using iron oxide tailings. *Water Research*, *38*(5), 1318-1326.

Appendix A

Equation 1: Concentration of Phosphate

$V1=[(1x10^{-6}mol/L)*(0.550L)/(0.008335mol/L)]$

$V1=(6.5x10^{-5}L)(1000ml/L)(1000ul/L)$

V1=66uL of NaH_2PO_4 solution to add

Table 4: Dithionite Extractions

Trial # **Sample**	**T1 (g)**	**T2 (g)**	**T3(g)**	**Average (g)**	**Standard Deviation**
Ferrihydrite	n/a	n/a	n/a	0.491	n/a
Ferrihydrite + Alginate	n/a	n/a	n/a	0.18233	n/a
Ferrihydrite + PO_4	10.2995	9.6594	9.6923	9.8837	0.3604
Ferrihydrite + Alginate + PO_4	31.63	33.494	44.278	36.468	6.8273

Inoculum Volume

This process was done in order to determine how much of the 100% CDM bacteria were to be added to the microcosm bottles. Three serial dilutions of 10x, 100x, and 1000x of the concentrated cell suspension were performed. 200 uL of BioRad Protein Assay was added to the various diluted cell suspensions, including the blank and brought to a final volume of 1000uL. After 5 minutes, the absorbance (at 595 nm) are measured and averaged and entered into equation 2**.** Where X is the volume of bacteria to

add to the bottle and is a theoretical amount that would give you an absorbance of 0.05, and 700mL is the amount of CDM in bottle. The value represents how much bacteria needed to be added to the microcosm bottles. Results are displayed in table 5.

Equation 2: Amount of bacteria added to microcosms

(Measured average absorbance)(XmL)=(0.05)(700mL)

Table 5: Inoculum Volume Added to Microcosms

Sample	**Amount *S. Putrefaciens* CN32 added (mL)**
Ferrihydrite	1.269
Ferrihydrite + Alginate	1.269
Ferrihydrite + PO_4	1.209
Ferrihydrite + Alginate + PO_4	1.06

Table 6: Sampling Times and Day for Reductions

Sample Time	**Fh**	**Fh + PO_4**	**Fh + Alginate**	**Fh + Alginate + PO_4**
T0	0	0	0	0
T1	2	2	2	2
T2	4	4	4	4
T3	6	6	6	6
T4	8	8	8	10
T5	10	10	10	12
T6	13	12	12	14
T7	15	14	14	16

T8	17	16	16	18
T9	n/a	20	n/a	20
T10	n/a	22	n/a	n/a

Calibration Curves

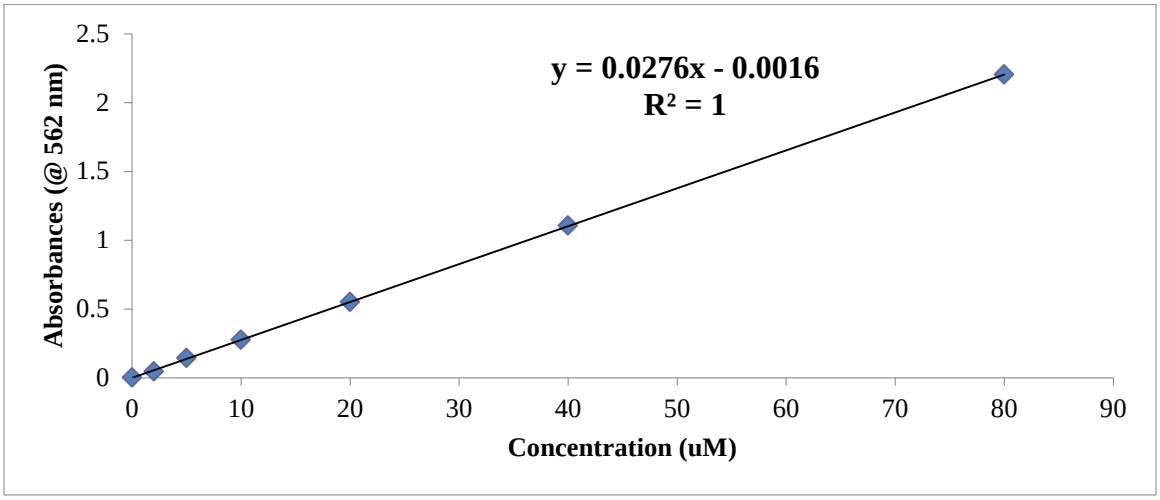

Figure 11: Ferrozine Calibration Curve for Fh and Fh+ Alginate Sample

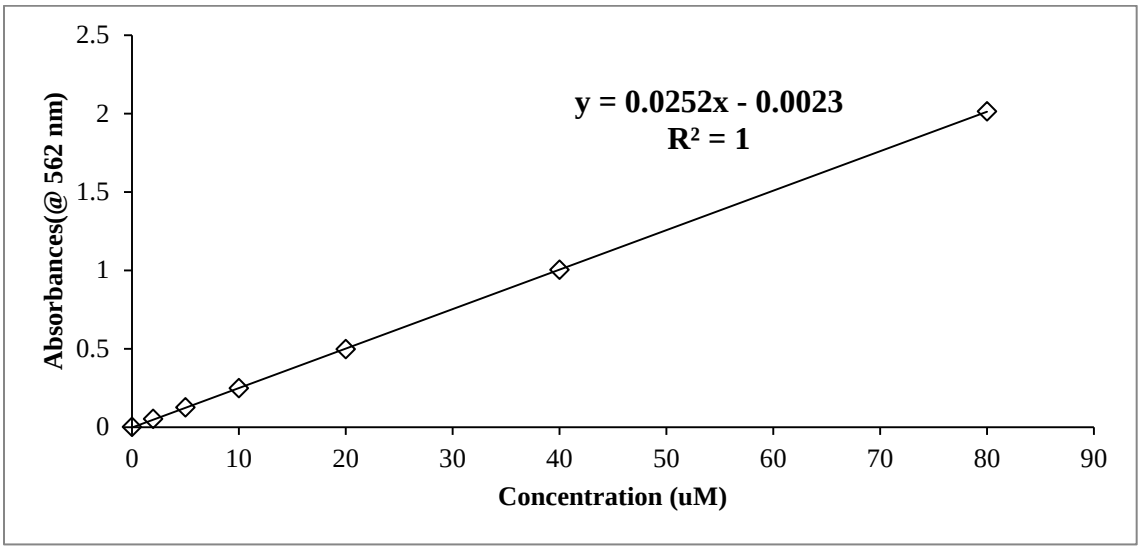

Figure 12: Ferrozine Calibration Curve for Fh + PO_4 and Fh + PO_4 + Alginate Samples

Fe(II)/Fe(III) Determination

In order to determine the molar ratio, and thus percentage of ferrous to ferric iron, the absorbance's from each sample time are converted into a concentration of iron in micromoles per litre(uM). When calculating the mM of iron for the Fe(II) and Fe(III) concentrations an equation for the line of best fit from the ferrozine calibration curves are used, which are shown above. The Fe(II) samples have a dilution factor of 500, 10x from chamber, and 46 from sample analysis which is rounded to 50x. The Fe(III) samples have a dilution factor of 1000. 10x from chamber, 10x from being in hydroxylamine + HEPES buffer solution, and then 10x for that sample being transferred into ferrozine. All trial points presented are an average of three trials, and the trend line displayed is a 3rd order polynomial line. Sample time T8 in the Ferrihydrite + alginate + PO_4 is missing data due to human error in experiment.

Equations for calculating concentration

Equation 3: Sample calculation for iron concentrations from Figure 11 (Fh and Fh+ Alginate samples)
$y = 0.0276x - 0.0016$

Y is a hypothetical absorbance of 0.005
$X(mM)=(0.005+0.016)/0.0276*1mM/1000uM*(dilution\ of\ 500\ or\ 1000)$
$X=7.610^{-4}*(dilution\ of\ 500\ or\ 1000)$

This same process is done using equation 4 for the samples containing phosphate (Fh + PO_4 and Fh+ alginate Sample + PO_4)

Equation 4: Sample calculation for iron concentrations from Figure 12 (Fh + PO_4 and Fh+Alginate + PO_4 samples)
$y =0.0252x-0.0023$

$X(mM)=(0.005+0.0023)/0.0252*1mM/1000uM*(dilution\ of\ 500\ or\ 1000)$
$X=2.9x10^{-4}*(dilution\ of\ 500\ or\ 1000)$

Rate of Reduction Calculations

In order to calculate the rate of reduction of Fe(III) to Fe(II), the slope of trend line of each trial is used taking the maximum and minimum points. Results are displayed in Table 2.

Table 7: Rate of Reduction Calculations

Sample	**Trial #**	**Calculation**	**Rate(mM Fe(II)/day**
Fh	1	=0.7083-0.1443/10-2	0.0705
	2	=0.7626-0.1354/15-2	0.0482
	3	=0.8324-0.1235/13-2	0.0644
Fh + Alg	1	=1.014-0.156/13-2	0.078
	2	=1.085-0.203/13-2	0.0801
	3	=1.032-0.219/13-2	0.0739
Fh + PO_4	1	=0.7913-0.0488/22-6	0.0464
	2	=0.8001-0.099/20-2	0.039
	3	=0.6174-0.0378/16-2	0.0414
Fh + Alg + PO_4	1	=0.361-0.0606/20-4	0.01878
	2	=0.3255-0.065/20-2	0.0145
	3	=0.2556-0.2017/20-14	0.00898

Cell Count Calculation

Converting a cell count to CFU/mL takes into account the amount plated, and the dilution factor of that sample. The sample count is divided by the amount plated, 0.1mL

and then that amount is divided by the overall dilution factor. Table 8 below displays the different equations, where # is the amount of colonies counted.

Table 8: Equations Converting Cell Count to CFU/mL at Various Dilutions

Dilution Factor	**Equation**
10^{-4}	(#/0.1mL)/(0.0001)
10^{-5}	(#/0.1mL)/(0.00001)
10^{-6}	(#/0.1mL)/(0.000001)